Hindawi
Shock and Vibration
Volume 2020, Article ID 8761278, 9 pages
https://doi.org/10.1155/2020/8761278

Research Article

Bearing Health Monitoring Based on the Orthogonal Empirical Mode Decomposition

C. Delprete, E. Brusa, C. Rosso, and F. Bruzzone

Department of Mechanical and Aerospace Engineering, Politecnico di Torino, Torino 10129, Italy

Correspondence should be addressed to C. Delprete; cristiana.delprete@polito.it

Received 30 July 2019; Revised 2 December 2019; Accepted 11 December 2019; Published 3 January 2020

Academic Editor: Dr Mahdi Mohammadpour

Bearing is a crucial component of industrial equipment, since any fault occurring in this system usually affects the functionality of the whole machine. To manage this problem, some currently available technologies enable the remote prognosis and diagnosis of bearings, before that faults compromise the system function and safety, respectively. A system for the in-service monitoring of bearing, to detect any inner fault or damage of components and material, allows preventing undesired machine stops. Moreover, it even helps in performing an out-monitoring action, aimed at revealing any anomalous behaviour of the system hosting bearings, through their dynamic response. The in-monitoring can be based on the vibration signal measurement and exploited to detect the presence of defects in material. In this paper, the orthogonal empirical mode decomposition is analysed and tested to investigate how it could be effectively exploited in a lean in-service monitoring operation and remote diagnosis. The proposed approach is validated on a test rig, where an elementary power transmission line was set up. The activity highlights some main properties and practical issues of the technological implementation, as well as the precision of the Orthogonal Empirical Mode Decomposition, as a compact approach for an effective detection of bearing faults in operation.

1. Introduction

The roller and ball bearings are crucial elements of rotating machinery, since they affect both the critical speeds and the dynamic stability of the supported shaft [1]. Failures occurring in the bearing system not only decrease its own life but even affect the performance of the whole rotor system in service. Unexpected overloading conditions, inadequate lubrication, or ineffective sealing [2] induce a wrong dynamic behaviour and may cause machine breakdowns, stops, and even dangerous accidents [3]. An effective fault diagnosis in rolling-element bearings assures both the system and workspace safety, as well as a continuous efficiency in production. Damage occurs in rolling elements, inner and outer raceways, and cages. Those different failures motivate the typical occurrence of a complex vibration signal which can be detected, monitored, and analysed. A series of impact impulses, for instance, is exhibited, when the rolling element impacts a localized fault [4, 5]. Luckily, the vibration signal induced by material damage arises at different frequencies. Therefore, dynamic analysis of monitored vibration can be exploited to perform the bearing diagnosis and even to localize the defect inside the damaged component [6].

Three main techniques have been assessed to perform the condition monitoring, based on the time-domain, the frequency-domain, and the time-frequency analyses [2, 6]. The first approach exploits the statistical interpretation of the vibration signal in time, to detect faults, which change some typical parameters of dynamic response [7–9]. The frequency-domain analysis is based on the elaboration of spectral contents of signal, as in the Fast Fourier Transform (FFT) [10]. The high frequency resonance analysis, referred to as "envelope analysis," identifies simultaneously the bearing fault and the affected element [11]. The envelope analysis has been widely applied, since 1974 [12], even in presence of pervasive noise, since it allows identifying the fault characteristic frequency, within the spectrum of vibration signal [13–15].

The early stage of defect nucleation is rather difficult to be detected through the first two approaches above

described, by monitoring the vibration signal, because of interference noise [16, 17]. The approach based on the combined time-frequency analysis looks more effective, because the interference noise is reduced, since this method works only on the frequency bandwidth of signal. Typical tools of the time-frequency analysis developed in the literature are the short-time Fourier transform, the wavelet transform [18–20], the spectral kurtosis [6, 21–23], and the Hilbert–Huang transform (HHT) [24–27].

The Empirical Mode Decomposition (EMD) is a self-adaptive time-frequency method, which detects the overlapping in time and in frequency by decomposing the nonstationary dynamic signal into several so-called "Intrinsic Mode Functions" (IMFs) [28]. This characteristic has been widely exploited in several fault diagnosis techniques [28–33]. Nevertheless, some drawbacks are still present, such as border effect evidence, unreliable stopping criterion [34, 35], and mode mixing. Those issues motivated a further development of the research activity, leading to some new refined approaches as the "Ensemble Empirical Mode Decomposition" (EEMD) [36, 37]. This method decomposes the dynamic signal by resorting to some noise assisted analysis technology [38–40], but it does not assure a precise identification of the IMFs [34]. Therefore, improving the EEMD has been performed by exploiting some statistical features [41]. Basically, the vibration signal is distinguished into noise, signal, and trend [42].

Particularly, the "Generalized Empirical Mode Decomposition" (GEMD) has been developed to comprehend the time-frequency-energy analysis and the features of the EMD and of its modified versions [43], while in some other case, the optimum frequency band was focalized [44]. The "Orthogonal Empirical Mode Decomposition" (OEMD) consists in a new procedure to decompose into IMFs, the monitored signals [45]. Multi-fault bearings have been tested in [46], and a new concept of EMD has been developed to select the most suitable IMFs to characterize the system faults.

According to the literature, the OEMD is fairly simply, user friendly, easy to be implemented, sufficiently fast, and precise, as well as easily implementable into a condition monitoring. Those properties are checked in a test case, to define the feasibility of exploiting this approach, in a complete system, especially when a smart monitoring based on a remote action of diagnosis and prognosis must be performed. The OEMD technique is here applied to a specific industrial case, to define the main needs of the monitoring system, and to check its effectiveness while testing. The experimental evidences confirm the effectiveness of the proposed approach, especially when results are compared with those of the envelope method, for a preliminary trade-off analysis of the in-monitoring system layout, as is done in the Model Based Systems Engineering [47]. Fulfilling requirements of the Industry 4.0 initiative, by introducing a bearing condition monitoring system in a simple and effective way is mandatory. Monitoring and data processing are performed to investigate the effectiveness of the proposed approach, and the suitability to be integrated within an industrial monitoring system, applied to several bearings, is explored.

2. Materials and Methods

To design the in-monitoring system, a preliminary description of the typical algorithms and methods applied to bearing dynamic signal is required, to develop and apply the Orthogonal Empirical Mode Decomposition.

2.1. The Hilbert–Huang Transform and the Empirical Mode Decomposition. Decomposing the bearing dynamic signal to define a series of Intrinsic Mode Functions (IMFs) and applying the Hilbert Transform is suggested in the time-frequency analysis. To describe this approach, it must be noticed that the IMFs satisfy two requirements; i.e., in the whole set of data, the difference between the number of extrema and the number of zero crossings must be equal or at least differ by one, and at any point of this function, the difference between the envelope of local maxima and of local minima must be null [48].

In the context of bearing dynamic analysis, the IMF should be considered as the dynamic signal, being characterized in amplitude and frequency. The majority of dynamic signals does not comply perfectly with the requirements of the IMFs. Therefore, if one just applies the Hilbert Transform, an accurate description of the instantaneous frequency of the bearing signal cannot be assured. However, it is possible decomposing first the signal into a sum of IMFs and then transforming the result through the Hilbert Transform.

Since a dynamic signal very seldom looks like an IMF, Huang et al. [24–26] proposed an adaptive approach to decompose the signal into IMFs because the decomposition is performed on the acquired dynamic signal, to interpret each mode separately as an IMF. Particularly, a generic signal, $h_1(t)$, is interpreted as the superposition of the acquired dynamic signal, $x(t)$, and an additional signal, $m(t)$, is expressively added, to fulfil the requirements to be an IMF. When a first mode is considered, that sum is

$$h_{1k}(t) = x(t) + m_1(t), \tag{1}$$

where k is the number of iterations required to complete the signal decomposition. Therefore, when function $h_{1k}(t)$ fulfils the requirements abovementioned to be an IMF, it is classified as the first IMF as follows:

$$c_1(t) = h_{1k}(t). \tag{2}$$

To reach that result, an iterative process is needed. The amplitude and frequency of the signal are not analysed separately, but the signal is taken as is. The iterative process uses different possible IMFs trying to minimize a defined stopping criterion. Usually, as in this paper, the standard deviation between two consecutive iterations, SD_k, is used as a criterion and kept within a threshold to stop the process:

$$\mathrm{SD}_k = \frac{\sum_{t=0}^{T} \left| h_{k-1}(t) - h_k(t) \right|^2}{\sum_{t=0}^{T} h_{k-1}^2}. \tag{3}$$

The first IMF $c_1(t)$ usually contains the highest frequencies present in the dynamic signal. A residual content is found as $r_1(t)$:

$$r_1(t) = x_1(t) - c_1(t). \tag{4}$$

The contribution of the remaining lowest frequencies is treated as a new signal. It is subjected to iteration process to extract the second IMF $c_2(t)$, and the procedure goes on, step by step, until that the whole signal is decomposed. This process is interrupted, when the last residual signal $r_n(t)$ becomes a monotonic function, a constant or an extreme function.

The above-described decomposition of the acquired dynamic signal into n modes is finally represented as

$$x(t) = \sum_{j=0}^{N} c_j(t) + r_n(t). \tag{5}$$

For each mode, it is possible to calculate the associated frequency.

2.2. Orthogonal Empirical Mode Decomposition. The Empirical Mode Decomposition (EMD) allows decomposing every dynamic signal into a finite number n of IMFs, as in equation (5). The energy associated to the oscillation modes of that decomposition is even found. For instance, when the signal $x(t)$ is decomposed into two IMFs:

$$x(t) = c_1(t) + c_2(t), \tag{6}$$

the total energy associated is [27]

$$E_x = \int_0^T x^2(t)\mathrm{d}t, \tag{7}$$

where T is the total duration of signal.

If the decomposition is performed with a negligible residual contribution $r(t)$, the energy can be calculated as a sum of the energies associated to the IMFs:

$$E_x = E_1 + E_2 = \int_0^T \left(c_1(t)\right)^2\mathrm{d}t + \int_0^T \left(c_2(t)\right)^2\mathrm{d}t. \tag{8}$$

According to equation (5), it can be even written as

$$E_x = \int_0^T \left(c_1(t) + c_2(t)\right)^2\mathrm{d}t. \tag{9}$$

Developing the content of integral in equation (9), it might be realized that equations (8) and (9) are equal only when the term with the product of functions $c_1(t)c_2(t)$ is null. This is possible, when the two IMFs are orthogonal. In this case, the two IMFs completely decompose the dynamic signal and precisely represent the energy associated. Similarly, this deduction can be applied to the n IMFs.

It can be noticed that the orthogonality of IMFs is theoretically demonstrated, but in practice it is never perfectly found, if the IMFs are identified by means of envelopes, obtained by cubic spline functions. This leads to an apparent loss of energy, when it is expressed by resorting to the IMFs. To investigate the real limitations of this method, a deeper investigation on the orthogonality of the IMFs is useful. Equation (5) can be expressed assuming that the residual signal $r(t)$ is an additional IMF:

$$x(t) = \sum_{j=1}^{n+1} c_j(t). \tag{10}$$

When the energy is calculated, the square value of signal is introduced:

$$x^2(t) = \sum_{j=1}^{n+1} c_j^2(t) + 2\sum_{j=1}^{n+1}\sum_{k=1}^{n+1} c_j(t)c_k(t). \tag{11}$$

If the orthogonality of modes holds, products at the right hand of equation (11) are null. To evaluate the degree of orthogonality exhibited by the system, an index can be defined:

$$\mathrm{OI} = \sum_{t=0}^{T} \frac{\sum_{j=1}^{n+1}\sum_{k=1}^{n+1} c_j(t)c_k(t)}{x^2(t)}. \tag{12}$$

It is referred to as orthogonality index (OI). Typical values span from 10^{-2} to 10^{-3}, when the energy lost by approximating the real content of the acquired signal by the IMFs is the minimum possible. If a lack of orthogonality is foreseen in the process, the symbol $\overline{c}_j(t)$ can be used to describe a generic nonorthogonal IMF. Whenever the first IMF is orthogonal and might be represented as OIMF (Orthogonal IMF), it is never assured that the second IMF is orthogonal to the first one. Therefore, when the second IMF is defined, at the end of the iterative process, it must be represented as

$$c_2(t) = \overline{c}_2(t) - \beta_{2,1}c_1(t), \tag{13}$$

where $\beta_{2,1}$ measures the percentage of $c_1(t)$ leading to overlapping between the two IMFs. Consequently, $\beta_{2,1}$ is defined as orthogonality coefficient between $\overline{c}_2(t)$ and $c_1(t)$. When this rationale is extended to the signal modes,

$$c_{j+1}(t) = \overline{c}_{j+1}(t) - \sum_{i=1}^{j} \beta_{j+1,i}c_i(t), \tag{14}$$

where $c_k(t)$ is the generic OIMF, with $k \le j$, which is orthogonal to all the other ones, when

$$\sum_{t=0}^{T} c_{j+1}(t)c_k(t) = 0. \tag{15}$$

Equations (14) and (15) can be used to formulate the orthogonality coefficient as

$$\beta_{j+1,i} = \frac{\sum_{t=0}^{T}\overline{c}_{j+1}(t)c_i(t)}{\sum_{t=0}^{T}c_i^2(t)}. \tag{16}$$

Therefore, the acquired dynamic signal can be composed by n IMFs and correlated as follows:

$$x(t) = \sum_{j=1}^{n}\left(c_j(t)\sum_{i=j}^{n}\beta_{i,j}\right) + r_n(t). \tag{17}$$

Introducing $a_j = \sum_{i=j}^{n}\beta_{i,j}$, it becomes

$$x(t) = \sum_{j=1}^{n} a_j c_j(t) + r_n(t) = \sum_{j=1}^{n} c_j^*(t) + r_n(t). \quad (18)$$

Equation (18) describes the acquired dynamic signal as the sum of n OIMFs, $c_j^*(t)$, and of residual signal, $r_n(t)$. The extraction of the IMFs has not been modified but resorting to orthogonal IMFs enhances this process. The OEMD assures the orthogonality of the IMFs, adding a powerful property to the decomposition of the monitored signal, but even preserves all the intrinsic characteristics of the IMFs.

2.3. Experimental Test Rig. Once that a protocol to process the dynamic signal is defined, by introducing the OEMD method, a test rig has been designed and built to test the approach, but even to analyse its practical implementation. Some main issues have been carefully considered:

(i) To set up all the required conditions for establishing a suitable analogy between a typical industrial equipment and this test rig

(ii) To implement a sufficiently wide variety of testing conditions even by resorting to a combination of different sources of vibration

(iii) To keep the assembly sufficiently simple to assure a repeatable and easy mounting

(iv) To design a structure to be tuneable through a known set of parameters

The test rig shown in Figure 1 reproduces at lower scale a quite typical industrial system. It consists in a power transmission line supported by rolling-element bearings and equipped with pulleys coupled by belts. Properties are described in Table 1.

The acquisition system is composed by two accelerometers PCB 308B ICP and a signal analyser DIFA-APB 200 (Table 2).

The frequencies of bearing defects are known in the literature. They depend on the defect itself, on the bearing type and angular speed [48]. They are classified and then used even in some industrial applications [49] to detect damages and predict the residual life of components. Some typical values of frequency are defined as

$$\begin{aligned} \text{BPFO} &= \frac{N}{2}\omega\left(1 - \frac{d}{D}\cos\theta\right), \\ \text{BPFI} &= \frac{N}{2}\omega\left(1 + \frac{d}{D}\cos\theta\right), \\ \text{BSF} &= \frac{N}{2}\omega\left(1 + \frac{d^2}{D^2}\cos^2\theta\right), \\ \text{FTF} &= \frac{1}{2}\omega\left(1 - \frac{d}{D}\cos\theta\right), \end{aligned} \quad (19)$$

where N is the number of rolling elements inside the bearing, ω the spin speed, d the diameter of rolling element, D the distribution diameter of the rolling elements, i.e., the average between the outer and inner diameter of bearing, and θ the contact angle between the rolling element and the raceways. The acronym BPFO stands for Ball Passing Frequency Outer, BPFI for Ball Passing Frequency Inner, BSF for Ball Spin Frequency, and FTF for Fundamental Train Frequency.

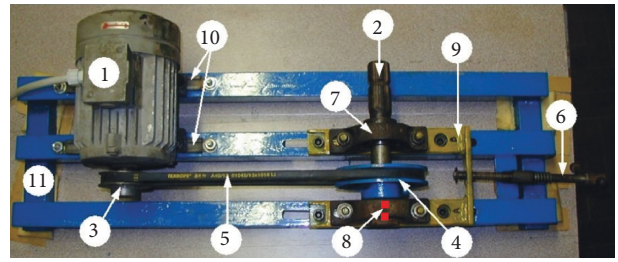

Figure 1: Test rig. 1, electric motor; 2, countershaft; 3, driving pulley; 4, driven pulley; 5, trapezoidal belt; 6, pretensioning system; 7, undamaged bearing; 8, faulty bearing; 9, positioning slide; 10, fixing rail for the electric motor; 11, platform. Red squares represent the two accelerometers mounted one vertical and one along the axis of the shaft.

When the damage nucleates and the fault arises, a series of impact impulses appears in the vibration spectrum of the machinery, as spikes in the signal, at one or even more values of frequency or of integer multiples of those. These marks include a defined information related to the type and location of damage. Considering the ball raceways (outer and inner), if a little crack appears, the frequency affected by irregularities in the spectrum of vibration is the BPFO (BPFI) or its fundamentals. If the size of defect increases, some lateral bands appear just in correspondence of that frequency. Their amplitude is related to the severity of defect. The spectrum becomes bevelled (spectrum comb). Considering defects on the balls, the affected frequency values are BSF and FTF and their fundamentals. The more the balls damaged, the higher the number of BSF fundamentals produced.

3. Results and Discussion

A preliminary validation of the orthogonal empirical mode decomposition (OEMD) method is performed by programming a dedicated MATLAB® code, and then results are compared with the data acquired on the test rig. When the shaft of test rig rotates at the typical spin speed of about 960 rpm, the synchronous signal is set at 16 Hz, and the characteristics frequencies of that bearing are 86 Hz (BPFO) and 57 Hz (BPFI).

Monitoring is performed by two accelerometers, being one (channel 1) aligned with the shaft axis and the other one (channel 2) along the radial direction of the monitored bearing. The monitoring activity includes some steps. A preliminary data acquisition in time is performed through channels 1 and 2, respectively. The data processing then starts and the OEMD method is applied. The OIMFs are extracted, and then the Fast Fourier Transform is applied to the interpreted signal based on the OIMFs. Finally, the data analysis is completed for the diagnosis of the system failures.

Table 1: Test rig main characteristics.

Electric motor	Asynchronous three-phase
	220 V 3.4 A Δ
	380 V 1.95 A Y
	$\cos\varphi = 0.79$
	P = 0.75 kW
	$\omega = 1400$ rpm
Bearings	SKF YAR 206-2F
	SY506M housing
Driving pulley	$\phi_i = 51$ mm
	$\phi_e = 78$ mm
Driven pulley	$\phi_i = 77$ mm
	$\phi_e = 106$ mm
First test rig natural frequencies	1° mode 300 Hz, 2° mode 1850 Hz, 3° mode 5800 Hz

Table 2: Accelerometers' main characteristics.

Voltage sensitivity	100 mV/g
Frequency range ±5%	1 ÷ 3000 Hz
Frequency range ±10%	0.7 ÷ 6500 Hz
Resonant frequency	≥22 kHz
Amplitude range	50 ± g pk
Resolution (broadband)	0.001 g rms
Temperature range	−65 ÷ 250°F
Amplitude linearity	±1%
Sampling frequency	25600 Hz

Firstly, the bearings without defects are tested, and then a defect is created in the outer and in the inner ring.

In Figure 2, a comparison of the harmonic content of the same bearing without and with defects is reported in order to highlight the very little difference and the necessity to use a detailed technique for understanding the presence of a defect.

In order to create defects, a trace inside the outer raceway was made by means of a tool with a sharp edge. By controlling the pressure on the tool, the trace can be created with different depths. The so-created defects can be easily characterized and measured. Tests were performed at different dimensions of the same defect, so starting with an invisible defect came to an important defect (order of 1/10 mm). The same procedure was used for damaging the inner ring.

3.1. Detection of Damage in the Outer Raceway. To test the monitoring system, some faults are intentionally created on bearings. A specific case study is here described as an example of the activity. A first defect is introduced in the outer raceway of monitored bearings with a dimension of 20 μm. The rotor system is then operated, and dynamic signals acquired on both the monitored channels. Each signal vector corresponding to a single channel is processed, by resorting to the OEMD method above described. Results are processed by the Fast Fourier Transform (FFT), which apply to each OIMF. As Table 3 shows, the OEMD method is able to detect the abovementioned characteristic frequency and some of its harmonics, by processing the data of both channels.

Figures 3 and 4 show some examples of the FFT obtained from the OIMFs. It can be noticed how evident is the

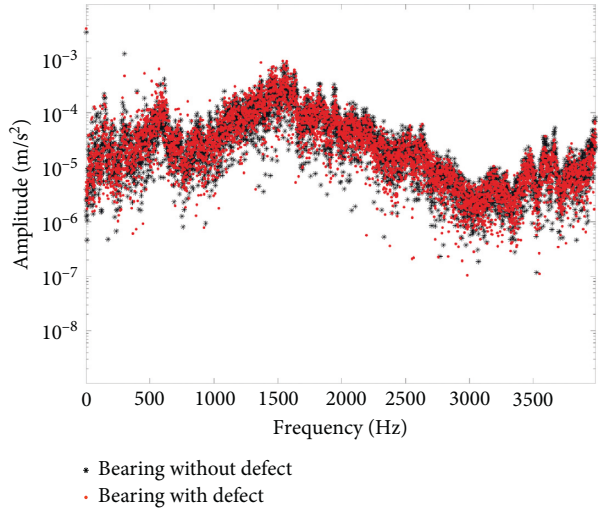

Figure 2: Harmonic content of the signals of bearing without and with defect.

Table 3: Detection of the defect in the outer raceway (BPFO), based on the data processing of channels 1 and 2; list of detected harmonics.

BPFO and its harmonics: channel 1		BPFO and its harmonics: channel 2	
1st OIMF	26 × BPFO 24 × BPFO 21 × BPFO 14 × BPFO	1st OIMF	14 × BPFO 12 × BPFO
2nd OIMF	14 × BPFO 10 × BPFO	2nd OIMF	14 × BPFO 12 × BPFO
3rd OIMF	10 × BPFO 8 × BPFO 5 × BPFO	3rd OIMF	14 × BPFO 12 × BPFO 8 × BPFO 6 × BPFO 5 × BPFO
4th OIMF	5 × BPFO 3 × BPFO	4th OIMF	6 × BPFO 5 × BPFO 3 × BPFO
5th OIMF	3 × BPFO 2 × BPFO	5th OIMF	3 × BPFO 2 × BPFO BPFO
6th OIMF	BPFO	6th OIMF	BPFO
7th OIMF	BPFO	7th OIMF	BPFO

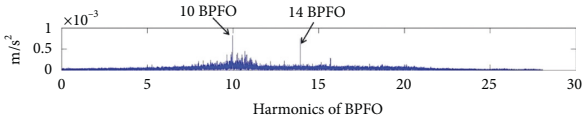

Figure 3: Defect on the outer raceway: channel 1, 2nd OIMF related to the BPFO.

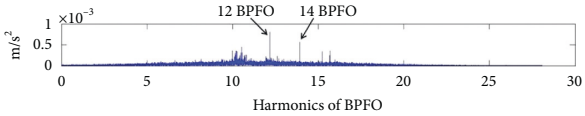

Figure 4: Defect on the outer raceway: channel 2, 2nd OIMF related to the BPFO.

spike associated to the characteristic frequency of defect and of its harmonics.

As results demonstrate, the OEMD detects the characteristic frequency of the induced defect on the outer ring, although its dimension is fairly small, if compared to other more evident damages [50]. The detection of super-harmonics of the base frequency improve the capability of detection, resolution of detected frequency is suitable for a precise detection, and moreover those results looked repeatable as the acquisition is performed several times within the same experimental campaign.

3.2. Detection of Defect in the Inner Raceway. The approach above described is applied to detect a defect induced in the inner raceway. In this case, the inner ring rotates together with the shaft. The defect is again artificially created, respecting the small dimensions to describe the incipient damage, with same size of that induced in the outer ring. As done for the outer ring, the acquired signal is decomposed into IMFs and residual signal, by the EMD method. The orthogonalization process is then applied.

Table 4 demonstrates that the OEMD method is able to detect the characteristic frequency of defect and related harmonics. Particularly, peaks in Figures 5 and 6 identify the defect.

3.3. Trade-Off of Defect Detection Approaches. The OEMD and the envelope methods are both applied to the test rig operation, even on dynamic signals acquired when the bearing SKF 1205 ETN9 is tested. The inner and outer raceways have been treated to simulate three levels of damage (20 μm, 60 μm, 100 μm). Dynamic signals are acquired along three directions by three-axes accelerometers. A comparison between the two methods can be performed. They both detect the faults introduced within the component material, despite the size quite small. At least some harmonics, multiple of the base one related with the fault induced, are found. Practically, the number of evident peaks is similar in the spectra elaborated by the two abovementioned methods. A better recognition of fault in both those cases is observed on the outer raceway, i.e., on the fixed and bigger ring. Nevertheless, even faults in the

Table 4: Detection of the defect in the inner raceway (BPFI), based on the data processing of channels 1 and 2; list of detected harmonics.

BPFI and its harmonics: channel 1		BPFI and its harmonics: channel 2	
1st OIMF	21 × BPFI	1st OIMF	20 × BPFI
	18 × BPFI		
	13 × BPFI		19 × BPFI
	10 × BPFI		
2nd OIMF	15 × BPFI	2nd OIMF	11 × BPFI
	14 × BPFI		10 × BPFI
	13 × BPFI		9 × BPFI
	12 × BPFI		
	10 × BPFI		
4th OIMF	5 × BPFI	3rd OIMF	9 × BPFI
	4 × BPFI		7 × BPFI
	8 × BPFI		
	6 × BPFI		
	5 × BPFI		
7th OIMF	BPFI	4th OIMF	9 × BPFI
		7th OIMF	BPFI

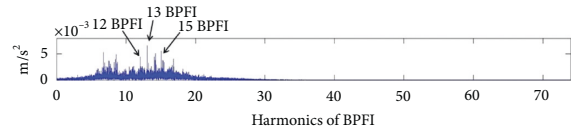

Figure 5: Defect on the inner race: channel 1, 2nd OIMF, referred to the BPFI.

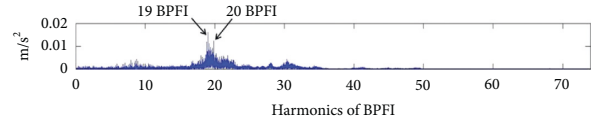

Figure 6: Defect on the inner race: channel 2, 1st OIMF, referred to the BPFI.

inner raceway are successfully detected. In terms of detection capabilities, both the envelope and OEMD methods are effective. The brightness of detection evidence is better in the OEMD because of the signal amplitude. In Figure 7, the comparison between results provided by the two methods is shown for the case of defect equal to 20 μm on the inner and outer rings; it can be noticed that the maximum value of dynamic signal at inner raceway is smaller, while at outer raceway is larger. The envelope and OEMD methods show a different response, depending on the type of fault. Results obtained through the OEMD method exhibit an average amplitude higher of 19% than the signal of the envelope method, considering the inner raceway and up to 29.5% higher for the outer raceway, for given fault.

The OEMD method looks effective in detection, compact in programming since the code can be easily stored and operated by a light computing device, the evidences of faults are bright because of the harmonics detected and of their amplitude, slightly larger than in the envelope method. The OEMD method is sensitive for incipient faults, even of small

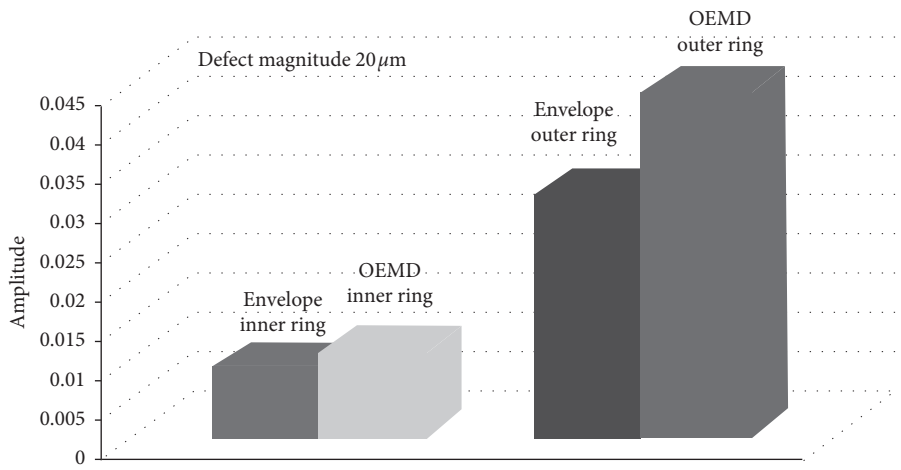

Figure 7: Comparison between the envelope and OEMD methods for inner ring and outer ring faults.

size like 20 μm. Signal-to-noise ratio is better for the OEMD method, and thus a higher capability of identifying the defect in presence of higher environmental noise has been found. The envelope method offers a lower accuracy for a smaller computational effort. However, for the in-monitoring service, the computational effort and time of the OEMD are largely compatible with the required operation.

4. Conclusion

Designing a lean in-monitoring system to early detect faults in inner and outer raceways of bearing is a current demand of industry. Technologies to perform an effective data acquisition and sensors to detect dynamic signals are currently available. The effectiveness of the damage detection depends on the data processing, both in terms of management and algorithms for the identification of faults. This issue motivates an investigation about the effectiveness of some diagnosis methods applied to the dynamic signal monitored on bearing as the orthogonal empirical mode decomposition (OEMD) method and the envelope method, both implementing a time-frequency analysis.

This study practically tested in a real case those methods and proposes a trade-off analysis. It is known that, in fault detection, noise interference reduces the effectiveness of diagnosis. Resolution of the method is even a relevant issue. Capability of identifying the fault and its location within the bearing is a crucial target. The experimental test campaign performed demonstrated that implementation of the OEMD method as well as the envelope method is fairly easy. Faults are identified even when smaller, on both the inner and outer raceways, through the identification of the characteristic frequency and its harmonics with a good approximation. Some comparative tests show that the amplitude of the signal harmonics decreases with the level of defect but is higher with the implementation of the OEMD method. This remark motivates resorting to the OEMD method, more than to the envelope method, despite the slightly higher computational effort, because of the more precise identification of fault, even when incipient.

Nomenclature

FFT:	Fast Fourier transform
HHT:	Hilbert–Huang transform
EMD:	Empirical mode decomposition
IMF:	Intrinsic mode function
EEMD:	Ensemble empirical mode decomposition
GEMD:	Generalized empirical mode decomposition
OEMD:	Orthogonal empirical mode decomposition
OIMF:	Orthogonal intrinsic mode function
$h_i(t)$, $x(t)$, $m(t)$:	Signals
$c_i(t)$:	i^{th} IMF
$r_i(t)$:	Residual
SD:	Standard deviation
E_i:	Signal energy
OI:	Orthogonality index
β:	Scale factor
N:	Number of rolling elements
ω:	Spin speed
D, d:	Characteristic diameters of bearings
θ:	Contact angle between rolling elements.

Data Availability

Data will be made available on demand if required.

Conflicts of Interest

The authors declare that they have no conflicts of interest.

References

[1] G. Genta, *Dynamics of Rotating Systems*, Springer, New York, NY, USA, 2005.

[2] I. Howard, "A review of rolling element bearing vibration—detection, diagnosis and prognosis," Technical Report, DSTO Aeronautical and Maritime Research Laboratory, Melbourne, Australia, 1994.

[3] D. Wang, P. W. Tse, and K. L. Tsui, "An enhanced kurtogram method for fault diagnosis of rolling element bearings,"

Mechanical Systems and Signal Processing, vol. 35, no. 1-2, pp. 179–199, 2013.

[4] R. B. Randall and J. Antoni, "Rolling element bearing diagnostics—a tutorial," *Mechanical Systems and Signal Processing*, vol. 25, no. 2, pp. 485–520, 2011.

[5] Y. Lei, J. Lin, Z. He, and Y. Zi, "Application of an improved kurtogram method for fault diagnosis of rolling element bearings," *Mechanical Systems and Signal Processing*, vol. 25, no. 5, pp. 1738–1749, 2011.

[6] A. Mohanty, *Machinery Condition Monitoring: Principles and Practices*, CRC Press, Boca Raton, FL, USA, 2005.

[7] P. D. McFadden and J. D. Smith, "Vibration monitoring of rolling element bearings by the high-frequency resonance technique—a review," *Tribology International*, vol. 17, no. 1, pp. 3–10, 1984.

[8] R. B. W. Heng and M. J. M. Nor, "Statistical analysis of sound and vibration signals for monitoring rolling element bearing condition," *Applied Acoustics*, vol. 53, no. 1–3, pp. 211–226, 1998.

[9] C. Delprete, M. Milanesio, and C. Rosso, "Rolling bearing monitoring and damage detection methodology," *Applied Mechanics and Materials*, vol. 3-4, pp. 293–301, 2006.

[10] Q. Miao, L. Cong, and M. Pecht, "Identification of multiple characteristic components with high accuracy and resolution using the zoom interpolated discrete Fourier transform," *Measurement Science and Technology*, vol. 22, no. 5, Article ID 055701, 2011.

[11] P. D. McFadden and J. D. Smith, "Model for the vibration produced by a single point defect in a rolling element bearing," *Journal of Sound and Vibration*, vol. 96, no. 1, pp. 69–82, 1984.

[12] M. S. Darlow, R. H. Badgley, and G. W. Hogg, "Application of high frequency resonance techniques for bearing diagnosis in helicopter gearboxes," Technical Report, US Army Air Mobility Research and Development Laboratory, Fort Belvoir, VA, USA, 1974.

[13] J. S. Cheng, D. J. Yu, and Y. Yang, "The application of energy operator demodulation approach based on EMD in machinery fault diagnosis," *Mechanical Systems and Signal Processing*, vol. 21, no. 2, pp. 668–677, 2007.

[14] M. Feldman, "Hilbert transform in vibration analysis," *Mechanical Systems and Signal Processing*, vol. 25, no. 3, pp. 735–802, 2011.

[15] L. Garibaldi, A. Fasana, and S. Marchesiello, "An experimental rig for damage detection of rolling bearings," *Key Engineering Materials*, vol. 293-294, pp. 509–516, 2005.

[16] D. Ho and R. B. Randall, "Optimisation of bearing diagnostic techniques using simulated and actual bearing fault signals," *Mechanical Systems and Signal Processing*, vol. 14, no. 5, pp. 763–788, 2000.

[17] J. S. Luo, D. J. Yu, and M. Liang, "A kurtosis-guided adaptive demodulation technique for bearing fault detection based on tunable-Q wavelet transform," *Measurement Science and Technology*, vol. 24, no. 5, Article ID 055009, 2013.

[18] R. Rubini and U. Meneghetti, "Application of the envelope and wavelet transform analyses for the diagnosis of incipient faults in ball bearings," *Mechanical Systems and Signal Processing*, vol. 15, no. 2, pp. 287–302, 2001.

[19] Q. Miao and V. Makis, "Condition monitoring and classification of rotating machinery using wavelets and hidden Markov models," *Mechanical Systems and Signal Processing*, vol. 21, no. 2, pp. 840–855, 2007.

[20] D. Wang, Q. Miao, X. Fan, and H.-Z. Huang, "Rolling element bearing fault detection using an improved combination of Hilbert and Wavelet transforms," *Journal of Mechanical Science and Technology*, vol. 23, no. 12, pp. 3292–3301, 2009.

[21] J. Antoni, "Fast computation of the kurtogram for the detection of transient faults," *Mechanical Systems and Signal Processing*, vol. 21, no. 1, pp. 108–124, 2007.

[22] J. Antoni, "The spectral kurtosis: a useful tool for characterising non-stationary signals," *Mechanical Systems and Signal Processing*, vol. 20, no. 2, pp. 282–307, 2006.

[23] A. Fasana, S. Marchesiello, M. Pirra, L. Garibaldi, and A. Torri, "Spectral kurtosis against SVM for best frequency selection in bearing diagnostics," *Mécanique & Industries*, vol. 11, no. 6, pp. 489–494, 2010.

[24] N. E. Huang and S. S. P. Shen, *Hilbert-Huang Transform and Its Applications Interdisciplinary Mathematical Sciences*, World Scientific Publishing, Singapore, 2005.

[25] R. Yan and R. X. Gao, "Hilbert-Huang transform-based vibration signal analysis for machine health monitoring," *IEEE Transactions on Instrumentation and Measurement*, vol. 55, no. 6, pp. 2320–2329, 2006.

[26] N. E. Huang, Z. Shen, S. R. Long et al., "The empirical mode decomposition and the Hilbert spectrum for nonlinear and non-stationary time series analysis," *Proceedings of the Royal Society of London. Series A: Mathematical, Physical and Engineering Sciences*, vol. 454, no. 1971, pp. 903–995, 1998.

[27] M. Feldman, "Analytical basics of the EMD: two harmonics decomposition," *Mechanical Systems and Signal Processing*, vol. 23, no. 7, pp. 2059–2071, 2009.

[28] B. Liu, S. Riemenschneider, and Y. Xu, "Gearbox fault diagnosis using empirical mode decomposition and Hilbert spectrum," *Mechanical Systems and Signal Processing*, vol. 20, no. 3, pp. 718–734, 2006.

[29] S. J. Loutridis, "Damage detection in gear systems using empirical mode decomposition," *Engineering Structures*, vol. 26, no. 12, pp. 1833–1841, 2004.

[30] D. Yu, J. Cheng, and Y. Yang, "Application of EMD method and Hilbert spectrum to the fault diagnosis of roller bearings," *Mechanical Systems and Signal Processing*, vol. 19, no. 2, pp. 259–270, 2005.

[31] Q. Gao, C. Duan, H. Fan, and Q. Meng, "Rotating machine fault diagnosis using empirical mode decomposition," *Mechanical Systems and Signal Processing*, vol. 22, no. 5, pp. 1072–1081, 2008.

[32] M. Pirra, A. Fasana, L. Garibaldi, and S. Marchesiello, "Damage identification and external effects removal for roller bearing diagnosis," in *Proceedings of the PHM Conference Europe 2012*, Dresden, Germany, July 2012.

[33] M. Pirra, S. Marchesiello, A. Fasana, and L. Garibaldi, "External condition removal in bearing diagnosis through EMD and one-class SVM," in *Proceedings of the XVIIth Symposium Vibrations, Shocks et Bruit VISHNO (Vibrations, Shocks and Noise)*, Écully, France, June 2010.

[34] H. Dong, K. Qi, X. Chen, Y. Zi, Z. He, and B. Li, "Sifting process of EMD and its application in rolling element bearing fault diagnosis," *Journal of Mechanical Science and Technology*, vol. 23, no. 8, pp. 2000–2007, 2009.

[35] A. Tabrizi, L. Garibaldi, A. Fasana, and S. Marchesiello, "Influence of stopping criterion for sifting process of empirical mode decomposition technique (EMD) on roller bearing fault diagnosis," in *Proceedings of the 3rd International Conference on Condition Monitoring of Machinery in Non-Stationary Operations (CMMNO2013)*, Ferrara, Italy, May 2013.

[36] Z. Wu and N. E. Huang, "Ensemble empirical mode decomposition: a noise-assisted data analysis method," *Advances in Adaptive Data Analysis*, vol. 1, no. 1, pp. 1–41, 2009.
[37] H. K. Jiang, C. L. Li, and H. X. Li, "An improved EEMD with multiwavelet packet for rotating machinery multi-fault diagnosis," *Mechanical Systems and Signal Processing*, vol. 36, no. 2, pp. 225–239, 2013.
[38] Y. Lei, Z. He, and Y. Zi, "EEMD method and WNN for fault diagnosis of locomotive roller bearings," *Expert Systems with Applications*, vol. 38, no. 6, pp. 7334–7341, 2011.
[39] Z. Feng, M. Liang, Y. Zhang, and S. Hou, "Fault diagnosis for wind turbine planetary gearboxes via demodulation analysis based on ensemble empirical mode decomposition and energy separation," *Renewable Energy*, vol. 47, pp. 112–126, 2012.
[40] W. Guo and P. W. Tse, "A novel signal compression method based on optimal ensemble empirical mode decomposition for bearing vibration signals," *Journal of Sound and Vibration*, vol. 332, no. 2, pp. 423–441, 2013.
[41] H. K. Jiang, W. Zhu, W. Li, G. Chen, and G. Zhou, "Robust condition monitoring and fault diagnosis of rolling element bearings using improved EEMD and statistical features," *Measurement Science and Technology*, vol. 25, no. 2, Article ID 025003, 2014.
[42] J. Dybala and R. Zimroz, "Rolling bearing diagnosing method based on empirical mode decomposition of machine vibration signal," *Applied Acoustics*, vol. 77, pp. 195–203, 2014.
[43] J. Zheng, J. Cheng, and Y. Yang, "Generalized empirical mode decomposition and its applications to rolling element bearing fault diagnosis," *Mechanical Systems and Signal Processing*, vol. 40, no. 1, pp. 136–153, 2013.
[44] J. Tian, C. Morillo, and M. G. Pecht, "Rolling element bearing fault diagnosis using simulated annealing optimized spectral kurtosis," in *Proceedings of the IEEE Conference on Prognostics and Health Management (PHM)*, Gaithersburg, MD, USA, June 2013.
[45] Q. S. Ren, Q. Yi, and M. Y. Fang, "Fast implementation of orthogonal empirical mode decomposition and its application into singular signal detection," in *Proceedings of the IEEE International Conference on Signal Processing and Communications (ICSPC)*, Dubai, UAE, November 2007.
[46] M.-C. Pan and W.-C. Tsao, "Using appropriate IMFs for envelope analysis in multiple fault diagnosis of ball bearings," *International Journal of Mechanical Sciences*, vol. 69, pp. 114–124, 2013.
[47] E. Brusa, A. Calà, and D. Ferretto, *Systems Engineering and Its Application to Industrial Product Development*, Springer, Cham, Switzerland, 2018.
[48] N. Tandon and A. Choudhury, "A review of vibration and acoustic measurement methods for the detection of defects in rolling element bearings," *Tribology International*, vol. 32, no. 8, pp. 469–480, 1999.
[49] E. Brusa, L. Lemma, and D. Benasciutti, "Vibration analysis of a Sendzimir cold rolling mill and bearing fault detection," *Proceedings of the Institution of Mechanical Engineers, Part C: Journal of Mechanical Engineering Science*, vol. 224, no. 8, pp. 1645–1654, 2010.
[50] Z. Yang and L. Yang, "A new definition of the intrinsic mode function," *WASET International Journal of Mathematical and Computational Sciences*, vol. 3, no. 12, pp. 1144–1147, 2009.